Timoshenko Beam Finite Elements Using Trigonometric Basis Functions

G. R. Heppler*
University of Waterloo, Waterloo, Ontario, Canada
and
J. S. Hansen†
University of Toronto, Toronto, Ontario, Canada

A Timoshenko beam finite element is developed using trigonometric basis functions. The properties and performance of these new elements are explored through a series of illustrative problems that treat both straight and curved geometries. Both linear and nonlinear strain-displacement relations are employed in the formulation and comparison is made to results obtained from full, completely reduced, and partially reduced integration of polynomial basis functions of degree one through three. The results obtained in this work indicate that the trigonometric basis functions are a competitive alternative to polynomial basis functions with regard to accuracy and convergence and most importantly they possess a freedom from shear and membrane locking. The trigonometric basis functions also allow the recovery of rigid-body motions in the case of straight and circular arc curved beams.

Introduction

In previous papers,[1-3] the use of unconventional basis functions in Reissner[4-6] or Mindlin[7] plate/shell finite elements has been explored in the context of the recovery of rigid-body motions. Here, the study has been restricted to the application of trigonometric basis functions to Timoshenko beam finite elements in order to clearly examine the characteristics of these basis functions in terms of accuracy, convergence, shear locking, and membrane locking for both straight and curved beams in linear and nonlinear geometry formulations.

Previous beam finite-element work[8-12] has been done using trial functions that were not strictly polynomials. In these cases classical Bernoulli-Euler beam theory was used as the foundation of the finite-element models and trial functions were employed that combined both polynomial and trigonometric terms. As in the present work, the previous investigations were originally concerned with the rigid-body motion capabilities of curved shell finite elements. It should be noted that the previous formulations used trigonometric terms, along with polynomial terms, in the form of trial functions and not in the more convenient basis function form. Past results have been obtained for linear static,[8-9] linear dynamic,[10] and static large-deflection nonlinear geometry[11] problems. Different trial functions were used for each degree of freedom and comparisons to different forms of the trial functions were reported. Although differences were observed between the various forms of trial functions, in general, the results obtained with trial functions that included trigonometric terms were superior to those containing only polynomial terms.

Dawe[12] explored several different trial function forms for shallow-arch elements, but, except for noting the need to have trigonometric terms present in order to recover the rigid-body motion capability, none of the trial functions investigated contained trigonometric terms. In a later paper,[13] one of the trial functions studied included both polynomial and trigonometric terms; that work was not restricted to shallow arches but dealt with circular arches. Neither of these papers used Timoshenko beam theory and both concluded that quintic polynomial interpolation over the element was to be preferred to the other cases investigated. Interestingly enough, the argumentation leading to the initial decision to use quintic polynomial trial functions examines the Taylor series expansions of the sine and cosine terms that would be necessary for exact reproduction of a general rigid-body motion.

In a paper primarily devoted to plate bending, Hughes et al.[14] introduce the idea of selective reduced integration in calculating the stiffness matrix for a shear-deformable beam element. This was done in order to realize satisfactory performance from a low-order polynomial trial function formulation in problems where the transverse shear effects should be negligible. The inability of a fully integrated low-order polynomial shear-deformable element to treat problems of this nature is referred to as shear locking and is of major concern in elements formulated on Timoshenko's beam theory.

A thorough discussion of the shear locking phenomenon as it applies to polynomial-based Timoshenko beam finite elements is provided by Prathap and Bhashyam.[15] Furthermore, in the case of curved Timoshenko beam finite elements, the interaction of the membrane and bending components of the response have been shown to give rise to membrane locking[16,17] that also finds relief in selective reduced integration of the stiffness matrix. Membrane locking is an excessive bending stiffness in curved elements that results from the contribution of the membrane component being overestimated in the discrete analysis.

A very recent work by Tabarrok et al.[18] treats the general case of curved and twisted rods by using information obtained from the equilibrium, strain-displacement, and constitutive relations to include the capability of recovering rigid-body and constant-strain states in the trial functions. Examples included in the work illustrate that the use of geometrically exact elements yields superior results to the case where the structure is modelled with prismatic rod elements. It was further concluded that the satisfaction of the rigid-body requirements by the trial functions was essential in cases where there was pretwist of the rod.

Received March 2, 1987; presented as Paper 87-0843-CP at the AIAA/ASME/AHS/ASEE 28th Structures, Structural Dynamics, and Materials Conference, Monterey, CA, April 6-8, 1987; revision received Nov. 2, 1987.

*Assistant Professor, Systems Design Engineering. Member AIAA.
†Professor, Institute for Aerospace Studies. Member AIAA.

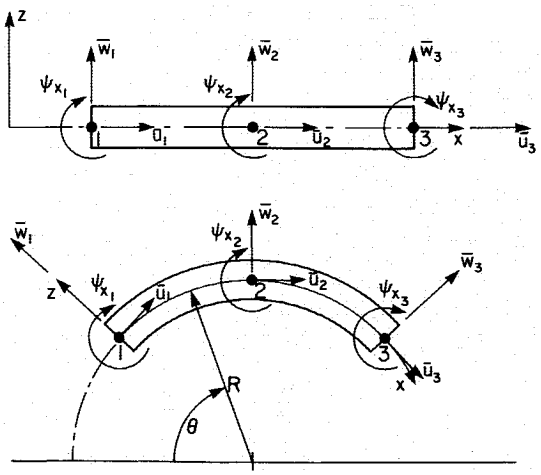

Fig. 1 Element geometry and nodal degrees of freedom.

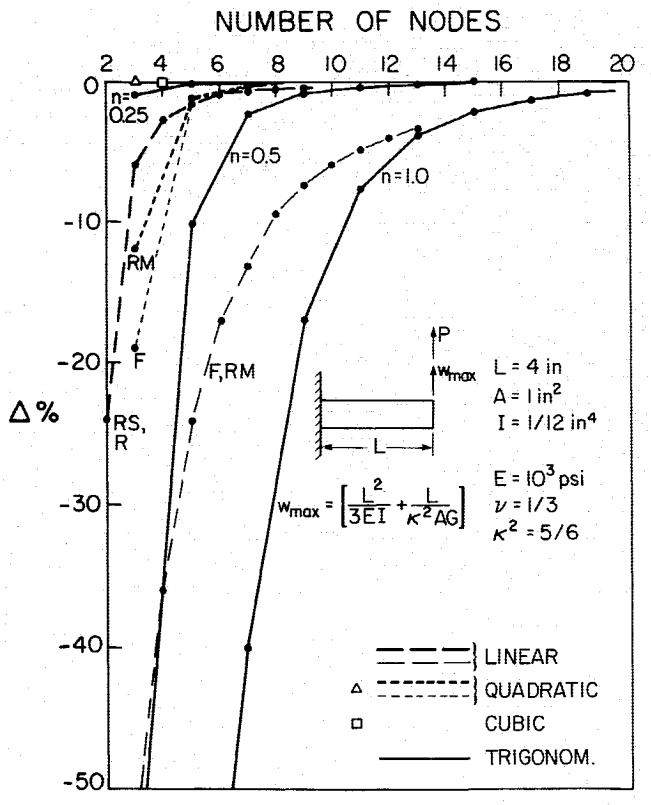

Fig. 2 Cantilever beam test: percentage difference between the analytical and the finite-element tip deflections, $L/h = 4$ (F = full integration; RS = reduced-shear integration; RM = reduced-membrane integration; and R = fully reduced integration).

Element Formulation

Timoshenko beam analysis can be considered to be the one-dimensional version of Reissner-Mindlin plate theory. Just as these plate theories have a wider range of applicability than Kirchhoff's thin-plate theory, Timoshenko beam theory has an extended range of application over the Bernoulli–Euler beam model. The inclusion of the transverse shear stress in the formulation allows treatment of deep beams (depth is large relative to length) but introduces some complications not found in the Bernoulli–Euler formulation. Principal among these is an inconsistency between the assumed form of the transverse shear stress and shear strain. That is, the usual assumptions on the displacements lead to, for example in straight beams, a constant shear strain. Whereas in order to satisfy the stress-free boundary conditions, the shear stress distribution is assumed to be quadratic. In order to resolve this inconsistency, the transverse shear strain is taken to be equal to the average shear stress on the cross section divided by the shear modulus and the shear correction factor κ^2. This gives rise to the question of what value should the shear correction factor take; the answer is best provided by Cowper.[19]

In order to treat curved as well as straight beams, curvilinear coordinates have been employed with the following nonlinear form of the strain-displacement relations:

$$\varepsilon_{xx} = \frac{1}{\alpha}\frac{\partial u}{\partial x} + \frac{w}{\alpha}\frac{\partial \alpha}{\partial z} + \frac{1}{2}\left(\frac{1}{\alpha}\frac{\partial w}{\partial x}\right)^2 \tag{1}$$

$$\gamma_{xz} = \frac{1}{\alpha}\frac{\partial w}{\partial x} + \frac{\partial u}{\partial z} - \frac{u}{\alpha}\frac{\partial \alpha}{\partial z} \tag{2}$$

where x, z are orthogonal curvilinear coordinates such that x lies along the neutral axis, or some other convenient reference line, such as the centroidal axis of the beam, and z is everywhere normal to the reference line. The tangential displacement u is in the x direction, while w is the normal deflection. The Lamé coefficient α is given by

$$\alpha = A(1 + C_x z) \tag{3}$$

with the curvature C_x, defined to be the reciprocal of the radius of curvature, that is, $C_x = 1/R_x$. As mentioned previously, the normal deflection is not to be allowed to vary over the depth of the beam, and there will be a rotation of the beam cross section that differs from the slope of the reference line. Thus, the displacements are taken to be in the form

$$u(x,z) = \bar{u}(x) + z\psi_x(x) \tag{4}$$

$$w(x,z) = \bar{w}(x) \tag{5}$$

where for $\bar{u}$ the superposed bar indicates a displacement at the reference line and $\bar{w}$ and ψ_x are the measures of normal deflection and rotation, respectively. Substitution of the expressions for u and w into the strain-displacement relations, Eqs. (1–2), results in strain expressions in terms of the rotation and displacement components given by

$$\varepsilon_{xx} = \frac{1}{\alpha}\left[\frac{\partial \bar{u}}{\partial x} + \bar{w}\frac{\partial \alpha}{\partial z} + z\left(\frac{\partial \psi_x}{\partial x}\right)\right] + \frac{1}{2}\left(\frac{1}{\alpha}\frac{\partial \bar{w}}{\partial x}\right)^2 \tag{6}$$

$$\gamma_{zx} = \frac{1}{\alpha}\left[\alpha\frac{\partial \bar{u}}{\partial z} + \frac{\partial \bar{w}}{\partial x} - \bar{u}\frac{\partial \alpha}{\partial z} + \alpha\psi_x - z\left(\psi_x\frac{\partial \alpha}{\partial z}\right)\right] \tag{7}$$

In a manner similar to that employed previously for shell elements,[20] the present formulation will not be restricted to thin shallow arches; this is achieved by expanding the factor $1/\alpha$ in the above, in a binomial series, which is subsequently truncated to terms of $O(z^2)$. This procedure results in the strain-displacement relations taking the form

$$\underline{\varepsilon} = \left[\sum_{i=0}^{2} B_{Li} z^i\right]\underline{d} + \frac{1}{2} B_N(\underline{d})\underline{d} \tag{8}$$

where

$$\underline{\varepsilon} = [\varepsilon_{xx}, \gamma_{zx}]^T, \qquad \underline{d} = [\bar{u}, \bar{w}, \psi_x]^T \tag{9}$$

and

$$\boldsymbol{B}_{L0}=\begin{bmatrix}\frac{1}{A}\frac{\partial}{\partial x} & C_x & 0\\ -C_x & \frac{1}{A}\frac{\partial}{\partial x} & 1\end{bmatrix},\quad \boldsymbol{B}_{L1}=\begin{bmatrix}-\frac{C_x}{A}\frac{\partial}{\partial x} & -C_x^2 & \frac{1}{A}\frac{\partial}{\partial x}\\ C_x^2 & -\frac{C_x}{A}\frac{\partial}{\partial x} & -C_x\end{bmatrix}$$

$$\boldsymbol{B}_{L2}=\begin{bmatrix}\frac{C_x^2}{A}\frac{\partial}{\partial x} & C_x^3 & \frac{-C_x}{A}\frac{\partial}{\partial x}\\ -C_x^3 & \frac{C_x^2}{A}\frac{\partial}{\partial x} & C_x^2\end{bmatrix} \tag{10}$$

The nonlinear part of the strain-displacement relations is treated in a way that simplifies the subsequent formation of the tangent stiffness matrix. The nonlinear terms are expressed as

$$\frac{1}{2}\boldsymbol{B}_N\underline{d}=\frac{1}{2}\left[\sum_{i=0}^{2}\boldsymbol{B}'_{Ni}z^i\right]\Phi\underline{d} \tag{11}$$

In the above, the $\boldsymbol{B}'_{Ni}$ arise from a binomial expansion of the $1/\alpha^2$ factor in Eq. (6) and hence

$$\boldsymbol{B}'_{N0}=\begin{bmatrix}\frac{1}{A^2}\frac{\partial\bar{w}}{\partial x}\\ 0\end{bmatrix},\quad \boldsymbol{B}'_{N1}=\begin{bmatrix}\frac{-2C_x}{A^2}\frac{\partial\bar{w}}{\partial x}\\ 0\end{bmatrix},\quad \boldsymbol{B}'_{N2}=\begin{bmatrix}\frac{3C_x^2}{A^2}\frac{\partial\bar{w}}{\partial x}\\ 0\end{bmatrix} \tag{12}$$

Basis Functions

The continuous displacements are replaced by a discrete approximation via the usual introduction of basis functions. The difference in this case, however, is that the basis functions of interest are not the usual polynomial basis functions, but still the general procedure holds. Because this formulation is not restricted to straight beams, all the degrees of freedom are to be modelled with the same order of basis function. Thus, the displacements are approximated by a suitable set of basis functions $\bar{N}_i$ such that the degrees of freedom at the ith node are $\bar{u}_i, \bar{w}_i, \psi_{xi}$ and the nodal displacement vector $\underline{d}_e$ is related to the continuous displacements $\underline{d}$ via the usual matrix of basis functions $\boldsymbol{N}$, such that $\underline{d}=\boldsymbol{N}\underline{d}_e$.

The original form of the trigonometric basis functions to be investigated in this paper was derived in Ref. 1 where they were given in terms of the angular position around a circular arc. However, it is often either necessary (as in the case of straight beams) or desirable to employ the curvilinear distance x in the formulation of the basis functions rather than the angular position θ. In this more versatile case the trigonometric basis functions take the following form:

$$\bar{N}_1(x)=\frac{\sin\left[\frac{2\pi n}{L}(x-x_2)\right]-\sin\left[\frac{2\pi n}{L}(x-x_3)\right]+\sin\left[\frac{2\pi n}{L}(x_2-x_3)\right]}{\sin\left[\frac{2\pi n}{L}(x_1-x_2)\right]-\sin\left[\frac{2\pi n}{L}(x_1-x_3)\right]+\sin\left[\frac{2\pi n}{L}(x_2-x_3)\right]} \tag{13}$$

where the second and third basis functions may be obtained by a cyclical permutation of the subscripts.[24] The quantity L is the total length of the finite-element model of the beam and n is a parameter that governs the wave content of the trial solution. The effect of this parameter is made clearer in the discussion of the results. The element is illustrated in Fig. 1 where the geometry and nodal coordinates are shown.

Substituting the discretized form of $\underline{d}$ into Eq. (8) and making use of Eq. (11), along with the fact that $\Phi\boldsymbol{N}=\boldsymbol{N}'$ (where the prime indicates differentiation with respect to x or equivalently θ), the strain-displacement relation can be ex-

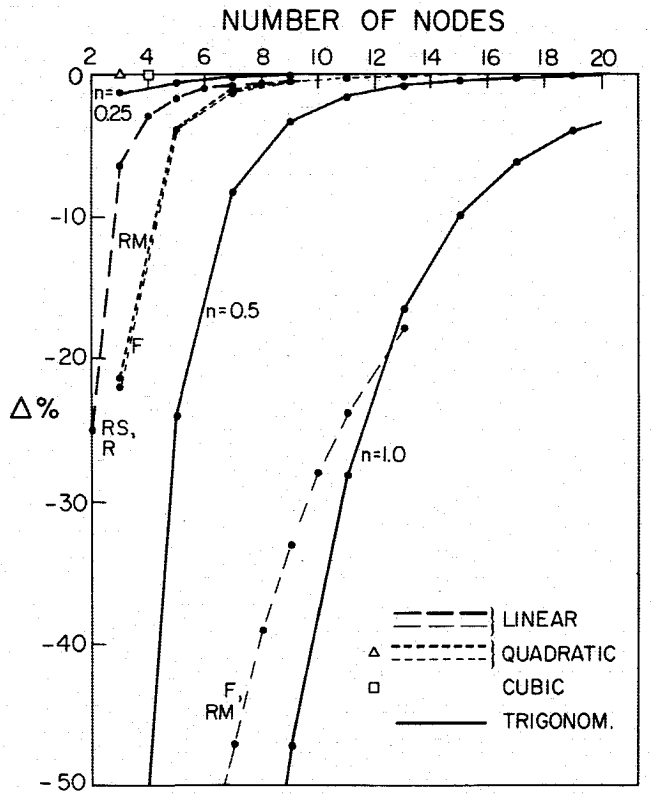

Fig. 3 Cantilever beam test: percentage difference between the analytical and the finite-element tip deflections, $L/h=10$.

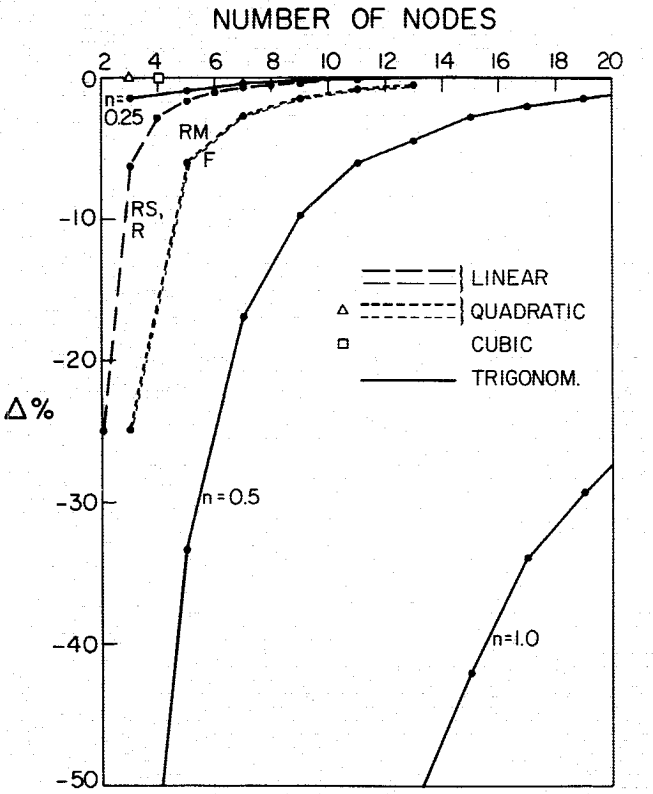

Fig. 4 Cantilever beam test: percentage difference between the analytical and the finite-element tip deflections, $L/h=50$.

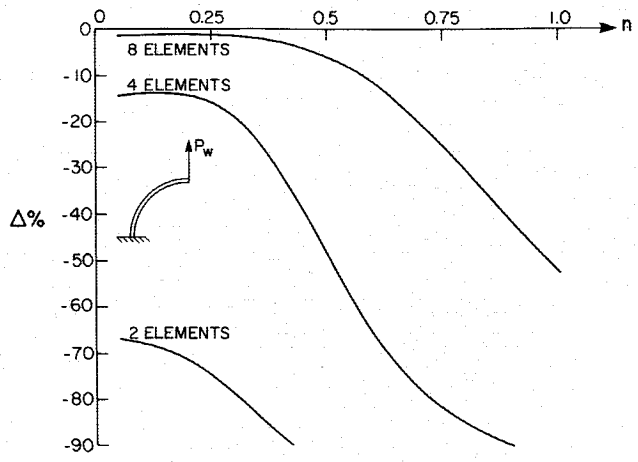

Fig. 5 Wave parameter n vs the percentage difference for two straight beam configurations.

pressed as

$$\underline{\varepsilon} = \left[\sum_{i=0}^{2} \boldsymbol{B}_{Li} z^i\right] \boldsymbol{N} \underline{d}_e + \frac{1}{2}\left[\sum_{i=0}^{2} \boldsymbol{B}'_{Ni} z^i\right] \boldsymbol{N}' \underline{d}_e \tag{14}$$

Constitutive Relations

For a homogeneous isotropic material and under the assumptions of Timoshenko beam theory, the constitutive operator can be shown to be

$$\boldsymbol{D} = \begin{bmatrix} E & 0 \\ 0 & \kappa^2 G \end{bmatrix} \tag{15}$$

The factor κ^2 introduced in the transverse shear term is the "shear correction factor" and may be determined from Cowper.[19]

Stiffness Matrix Formulation

Incorporating the strain-displacement and constitutive relations into the strain energy integral, it is found that the potential energy is given by

$$\begin{aligned} P.E. = \frac{1}{2}\int_V \Bigg[& \underline{d}_e^T \left(\sum_{i=0}^{2} \boldsymbol{B}_{Li} z^i\right)^T \boldsymbol{D} \left(\sum_{j=0}^{2} \boldsymbol{B}_{Lj} z^j\right) \underline{d}_e \\ & + \underline{d}_e^T \left(\frac{1}{2}\sum_{i=0}^{2} \boldsymbol{B}_{Ni}(\underline{d}_e) z^i\right)^T \boldsymbol{D} \left(\sum_{j=0}^{2} \boldsymbol{B}_{Lj} z^j\right) \underline{d}_e \\ & + \underline{d}_e^T \left(\sum_{i=0}^{2} \boldsymbol{B}_{Li} z^i\right)^T \boldsymbol{D} \left(\frac{1}{2}\sum_{j=0}^{2} \boldsymbol{B}_{Nj}(\underline{d}_e) z^j\right) \underline{d}_e \\ & + \underline{d}_e^T \left(\frac{1}{2}\sum_{i=0}^{2} \boldsymbol{B}_{Ni}(\underline{d}_e) z^i\right)^T \boldsymbol{D} \left(\frac{1}{2}\sum_{j=0}^{2} \boldsymbol{B}_{Nj}(\underline{d}_e) z^j\right) \underline{d}_e \Bigg] \mathrm{d}V - W \end{aligned} \tag{16}$$

where for a general arch $\mathrm{d}V = \alpha\, \mathrm{d}x\, \mathrm{d}y\, \mathrm{d}z$. Taking the first variation of the potential energy $P.E. = U - W$ leads to a nonlinear equilibrium equation of the form $\boldsymbol{N}(\underline{d}_e) = \underline{F}_e$ that is best solved incrementally by employing a linearized form of this equation. This leads to the usual tangent stiffness formulation. The first term in Eq. (16) yields the usual linear stiffness matrix $\boldsymbol{K}_0$, and the remaining terms lead to the nonlinear stiffness matrix $\boldsymbol{K}_N$ and the initial stress stiffness matrix $\boldsymbol{K}_\sigma$ that comprise the remainder of the tangent stiffness matrix. Specifically,

$$\boldsymbol{K}_T = \boldsymbol{K}_0 + \boldsymbol{K}_N + \boldsymbol{K}_\sigma \tag{17}$$

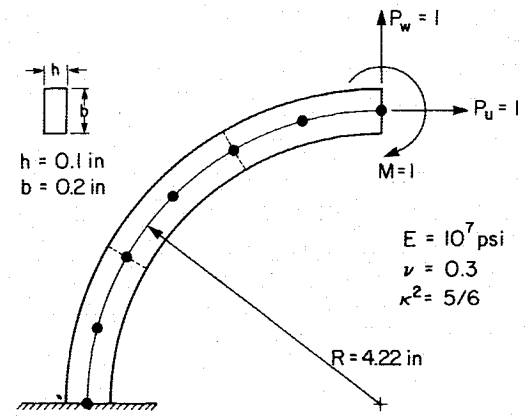

Fig. 6 Curved cantilever beam test geometry.

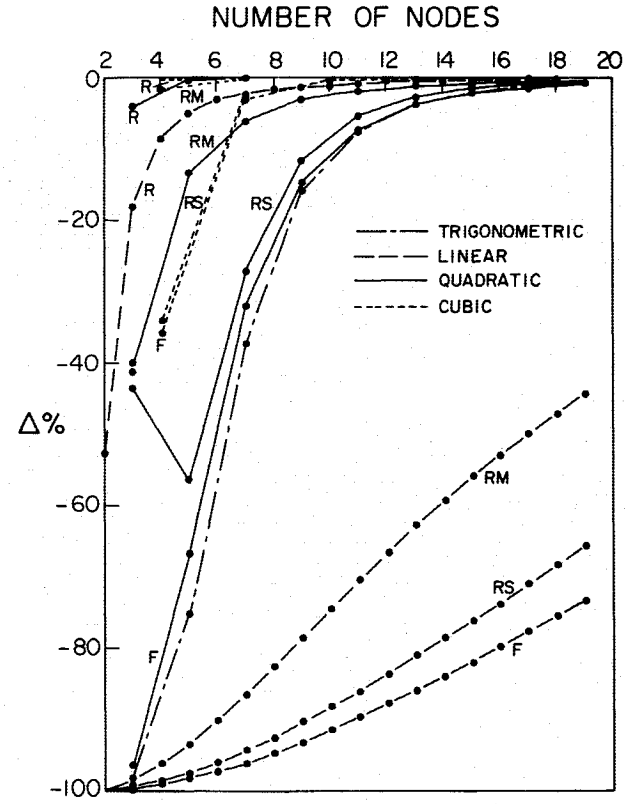

Fig. 7 Percentage difference between the analytical and the finite-element radial tip deflections under a unit radial tip load.

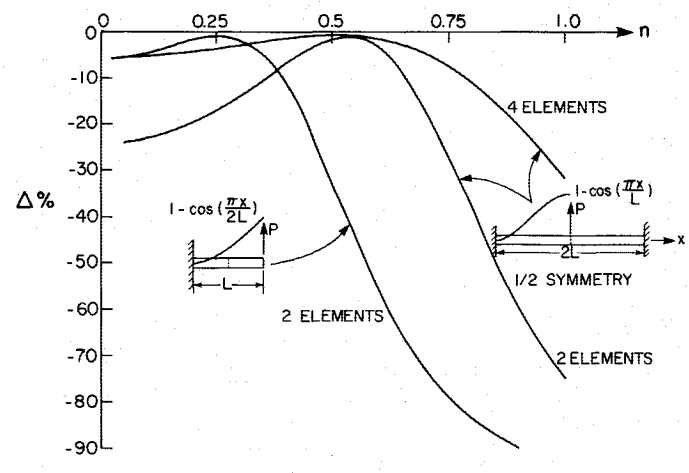

Fig. 8 Wave parameter n vs the percentage difference for the unit radial tip load.

The details of this procedure may be found in Pica et al.[21] or Heppler.[22]

In order that these beam elements could be used as stiffener elements on plates and shells, the reference line was not assumed to pass through the centroid of the beam cross section. This results in a more general but slightly more complicated formulation. To illustrate this technique, only the linear stiffness matrix term will be discussed; the means of treating the others follows directly.

From the first term in Eq. (16), the linear stiffness matrix may be expressed as

$$\boldsymbol{K}_0 = \int\int\int \left[\sum_{i=0}^{2} \sum_{j=0}^{2} \sum_{k=0}^{1} a_k (\boldsymbol{B}_L \boldsymbol{N})^T \boldsymbol{D} \boldsymbol{B}_L \boldsymbol{N} z^{i+j+k} \right] A \, dx \, dy \, dz \tag{18}$$

Note that $a_0 = 1$, $a_1 = C_x$, and that $dy\, dz$ can be replaced by dA_{yz}. This latter equivalence allows the use of

$$A_{yz} = \int\int dy\, dz, \qquad \bar{z} A_{yz} = \int\int z \, dy\, dz, \qquad I_{yy} = \int\int z^2 \, dy\, dz \tag{19}$$

in forming the stiffness matrix. Thus, by noting the degree of z in the integrand of Eq. (18) and not allowing it to exceed 2 (consistent with the truncation of the binomial expansion of α), the integral in Eq. (18) can be evaluated very easily and economically by specifying the beam's cross-sectional area, eccentricity of the centroid from the reference line, and the second moment of the area. The integration along the length of the beam is readily achieved by the method of Ref. 1, in the case of trigonometric basis functions, or by Gaussian quadrature in the case of polynomial basis functions.

The integration method for trigonometric basis functions developed in Ref. 1 assumed the use of angular coordinates rather than arc-length coordinates as presented in Eq. (13). For this latter case, the integration rule must be modified slightly.[24]

Tests and Results

As the first example, a series of cantilever beams with three length-to-depth ratios were considered, $L/h = (4,10,50)$. The beams were loaded by a single normal point load at the free end of the beam as illustrated in Fig. 2; the material and geometry data are as given.

In order to determine the convergence and accuracy of the trigonometric basis function formulation, comparison was made to the predicted tip deflection given by Roark and Young.[23] In addition to the results for the trigonometric basis function formulation, Fig. 2 also presents results obtained for linear, quadratic, and cubic polynomial basis functions under full, shear-reduced, membrane-reduced, and fully reduced integration schemes. It may be observed that the cubic polynomial basis functions yield zero error, for any number of elements, regardless of the order of integration used. This is because the analytical solution for the displacement field is a cubic polynomial in x and consequently it must be the case that the cubic basis functions yield the exact deflection. In addition, the exact result is also obtained with the quadratic basis functions when reduced shear or fully reduced integration is used. Membrane-reduced integration has no effect in this example due to the absence of curvature. These results are consistent with the findings of Prathap and Bhashyam.[15] In a similar way to the quadratic and cubic basis functions, shear-reduced integration or fully reduced integration improved the convergence rate for the linear elements, but a higher-order polynomial basis function would still be preferred.

The results obtained for the trigonometric basis functions illustrate that they can be superior to any of the polynomial basis functions except of course where the exact solution has

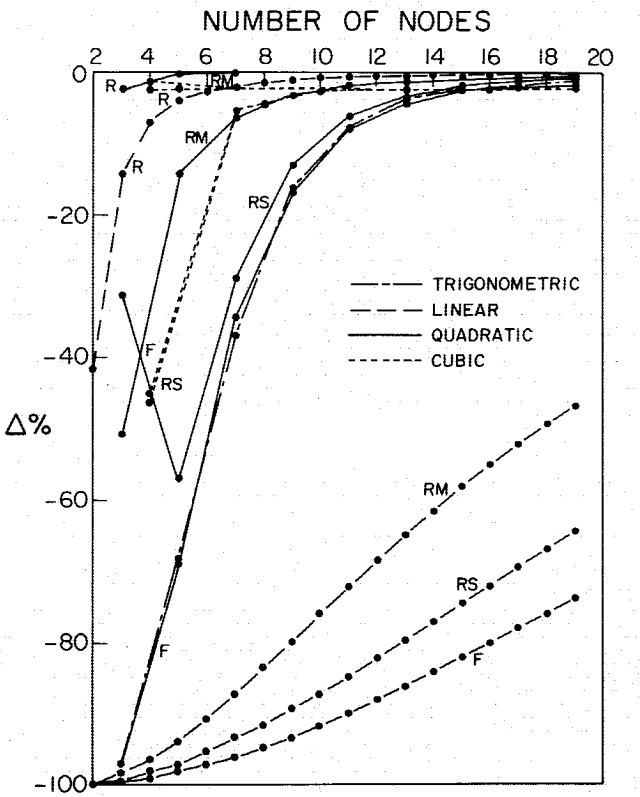

Fig. 9 Percentage difference between the analytical and the finite-element radial tip deflections under a unit tangential tip load (F = full integration; RS = reduced-shear integration; RM = reduced-membrane integration; and R = fully reduced integration).

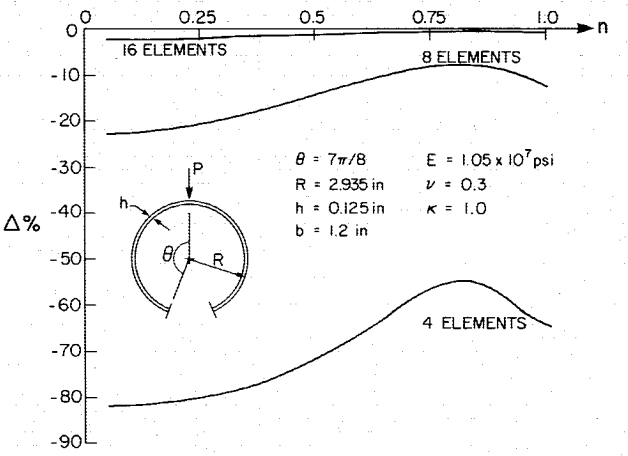

Fig. 10 Wave parameter n vs the percentage difference in the displacement under the applied load for a deep arch.

been achieved. Three sets of results are presented for the trigonometric basis functions, each corresponding to a different wave parameter n. The accuracy and convergence for $n = 0.25$ is excellent; more on this later.

Identical trends are exhibited in Figs. 3 and 4 where results for beams of $L/h = 10$ and $L/h = 50$ are presented. Results for fully integrated and membrane-reduced integration of the linear basis functions do not appear in Fig. 4 because the error in these results places them off the bottom of the graph, and it was not considered worthwhile to compress the vertical scale of the figure in order to include such poor results. It must be noted that the trigonometric basis functions do not display any shear locking behavior. On this point, the rational

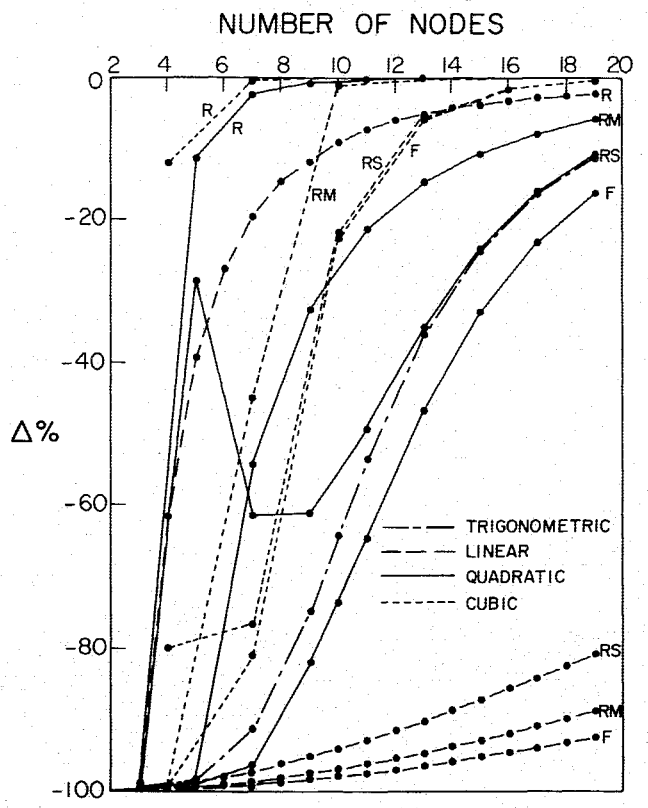

Fig. 11 Deep arch problem: percentage difference between the analytical and the finite-element radial deflections under the applied load.

given by Prathap and Bhashyam,[15] when applied to the trigonometric basis functions, indicates that they cannot lock.

The effect of the choice of wave parameter is shown in Fig. 5 for the cantilever beam and for a clamped-clamped beam under a center point load as illustrated. In the latter case, half symmetry was used in the finite-element model. The percentage disagreement between the finite-element results and the solution given by Roark and Young[23] is plotted against the value of n used in the trigonometric basis functions. For the cantilever beam the minimum error is realized for $n = 0.25$. This is due to the similarity of the sine and cosine functions over the interval 0 to $\pi/2$ to the final deformed shape of the beam, i.e., both have a zero slope and displacement at the root ($x = 0$) and some finite slope and displacement at the free end ($x = L$). By contrast, the shape of the sine and cosine functions over the interval 0 to 2π does not resemble the deformed shape of the cantilever at all and consequently far more elements are required to achieve a reasonable accuracy when $n = 1$ as compared to $n = 0.25$. This is borne out by the results for the clamped-clamped beam where the optimal wave parameter is found to be $n = 0.5$. To see why this wave parameter is best, consider the similarity in shape between $1 - \cos(2\pi nx/L)$, $x = [0,L]$, $n = 0.5$ and the expected deformation of half of the beam (Fig. 5).

The next test situation is that of a tip-loaded curved cantilever beam that covers one-quarter of a circular arc. The details of the geometry and material parameters are given in Fig. 6. Comparison to Roark and Young[23] is made in Figs. 7–9 where results are presented only for the radial deflection at the free end of the beam as the predicted tangential displacement and the slope show similar results.

The results for the trigonometric basis functions shown in Fig. 7 are for the form that allows recovery of the rigid-body motion capability.[1] It is apparent that the quadratic and cubic basis functions converge more rapidly than the trigonometric basis functions and that the linear basis functions, when completely under integrated, also perform better. When the

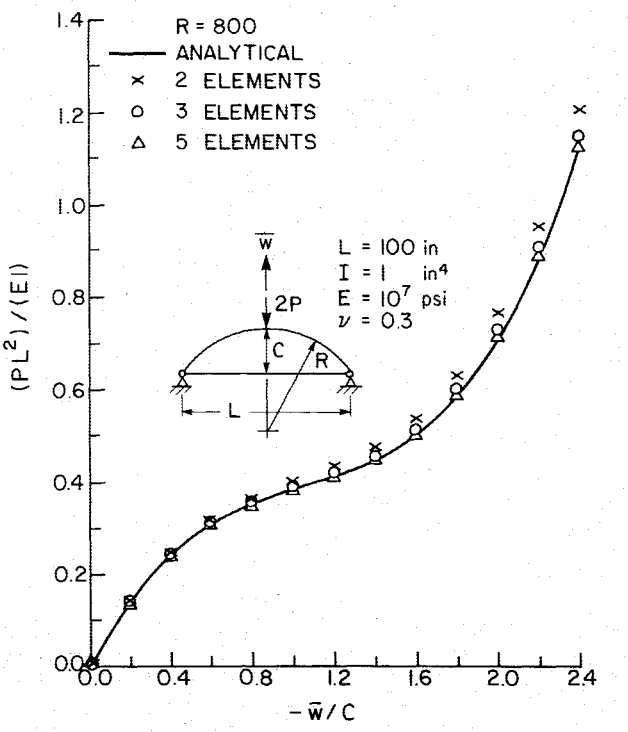

Fig. 12a Nonlinear analysis of a circular arch; trigonometric basis functions; $R = 800$ in.

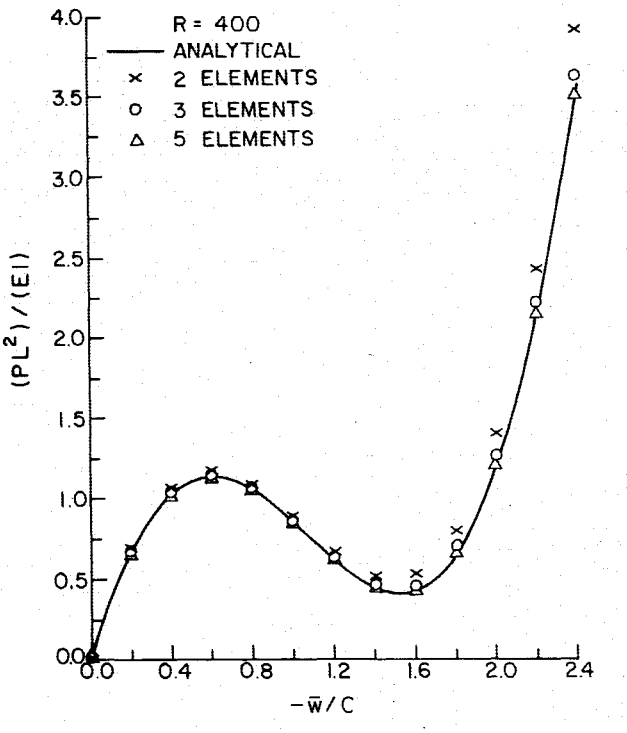

Fig. 12b Nonlinear analysis of a circular arch; trigonometric basis functions; $R = 400$ in.

form of the trigonometric basis functions presented in Eq. (13) is used in this situation, the results shown in Fig. 8 are achieved. These show that the value of n that corresponds to that required to achieve rigid-body motion capability in the basis functions results in minimum error. However, it is also the case that this value of n is optimal for cantilever configurations as illustrated in the previous example. Finally, there is no indication of either shear or membrane locking with the

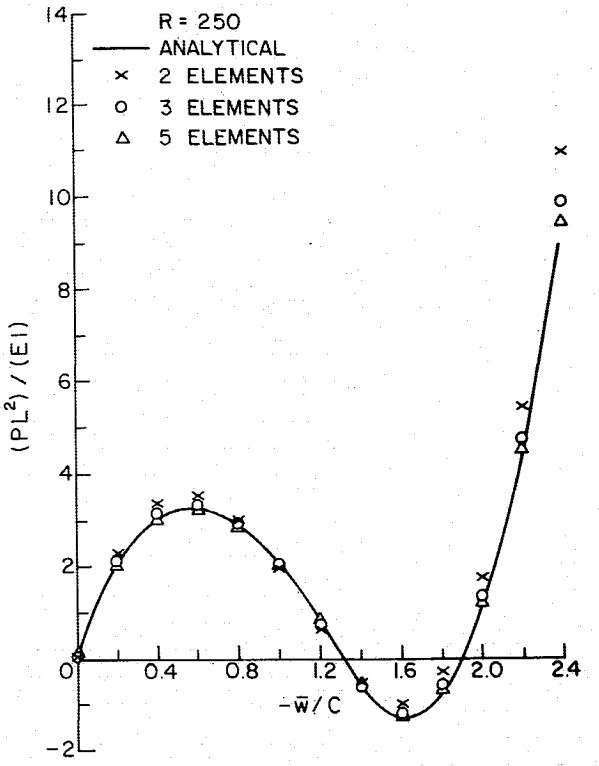

Fig. 12c Nonlinear analysis of a circular arch; trigonometric basis functions; $R = 250$ in.

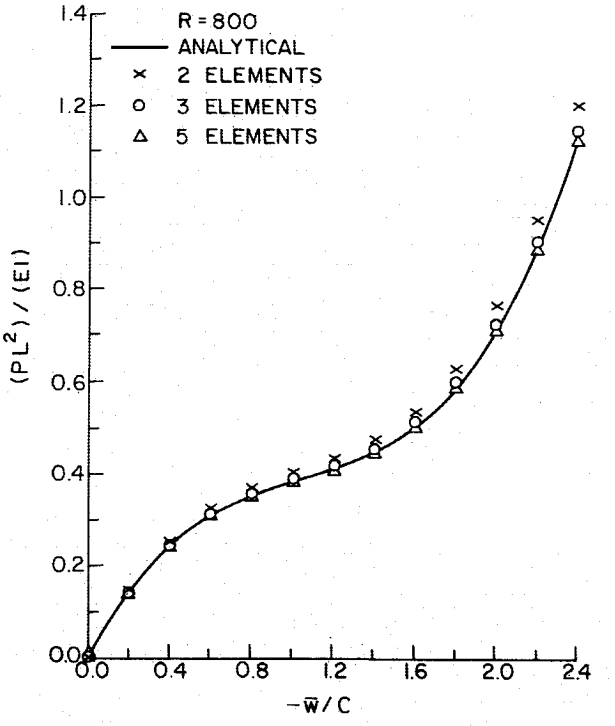

Fig. 13 Nonlinear analysis of a circular arch; quadratic basis functions, full integration; $R = 800$ in.

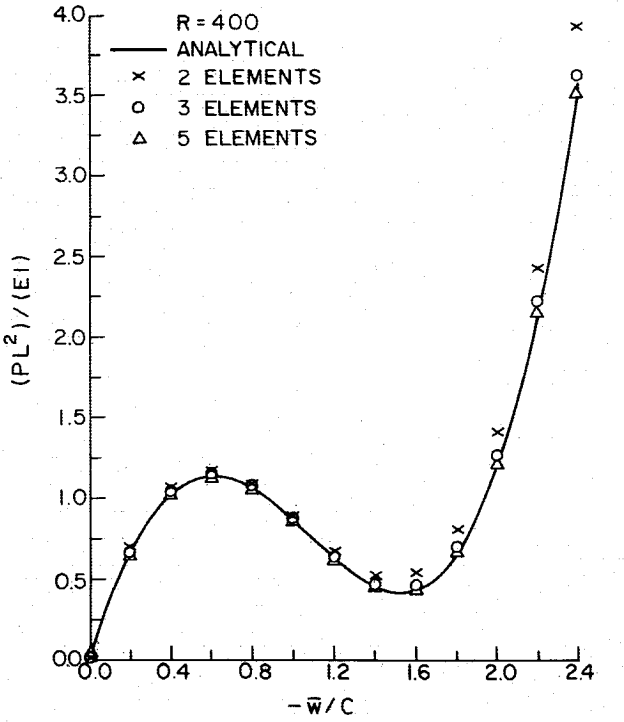

Fig. 14 Nonlinear analysis of a circular arch; quadratic basis functions, full integration; $R = 400$ in.

trigonometric basis functions that, it must be emphasized, are fully integrated.

The results obtained for the tangential force, Fig. 9, show similar accuracy and convergence characteristics to those presented in Fig. 7. Of note in Figs. 7 and 9 is the behavior of the quadratic elements when shear-reduced integration is used. A single element appears to be far more flexible, in terms of the tip deflection, than an assembly of elements. Results for a unit moment applied at the tip may be found in Ref. 24.

As a final linear example, the deep arch illustrated in Fig. 10 was treated. In this same figure, the results of varying n as used in Eq. (13) are reported. Half symmetry was used in constructing the finite-element model, and convergence to within 0.7% of the analytical answer[23] is achieved with a mesh of 16 elements and $n \approx 0.8$. The trigonometric basis functions as given in Ref. 1 correspond to a value of $n = 0.4375$, and these are compared to results obtained from the polynomial basis functions in Fig. 11. All versions of the cubic basis function formulation and all but the fully integrated quadratic formulation exhibit superior convergence to the basic trigonometric formulation. As in the previous example, the behavior of the quadratic element that uses shear-reduced integration is anomalous in comparison to the results achieved with the other polynomial basis functions. In this example, the optimal value of n is not intuitively obvious and would suggest that the possibility of including this parameter as one of the generalized coordinates in the trial function form of these basis functions may be in order. Unfortunately, this would result in turning the solution for the generalized coordinates into a nonlinear problem, the solution to which may require more effort than is worth expending for the end result. It would most certainly represent a major divergence from the usual and straightforward finite-element formulation method.

The application of these elements to nonlinear problems is illustrated in the following examples. The problem geometry is given in Fig. 12 and consists of a simply supported circular arch subjected to a point load. An exact solution was obtained by applying the method used by Schreyer and Masur[25] and is used for comparison purposes. Three arches of differing radii were used with each displaying a fundamentally different behavior ranging from no buckling to buckling with load sign reversal. Only half of the arch was modelled, thereby forcing symmetric deformations, and the results were obtained for prescribed deflection increments with the reaction load at the top of the arch being the quantity to be determined. It was the

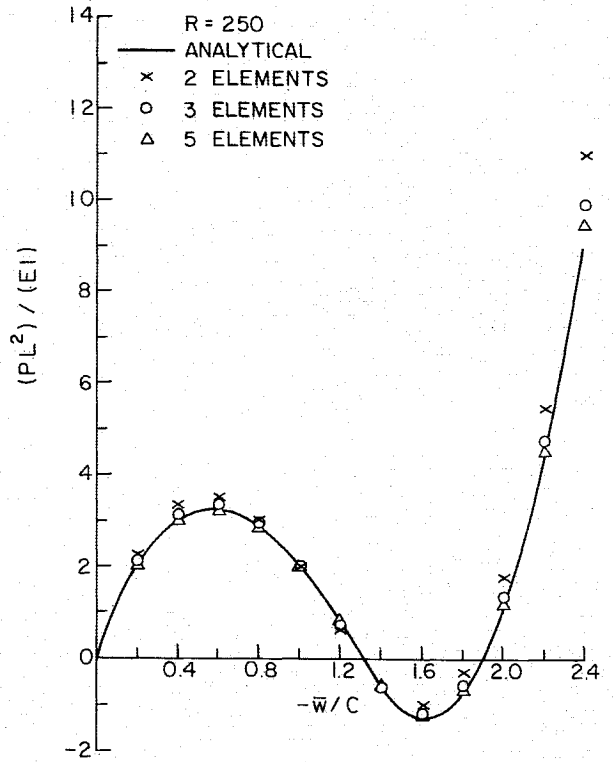

Fig. 15 Nonlinear analysis of a circular arch; quadratic basis functions, full integration; $R = 250$ in.

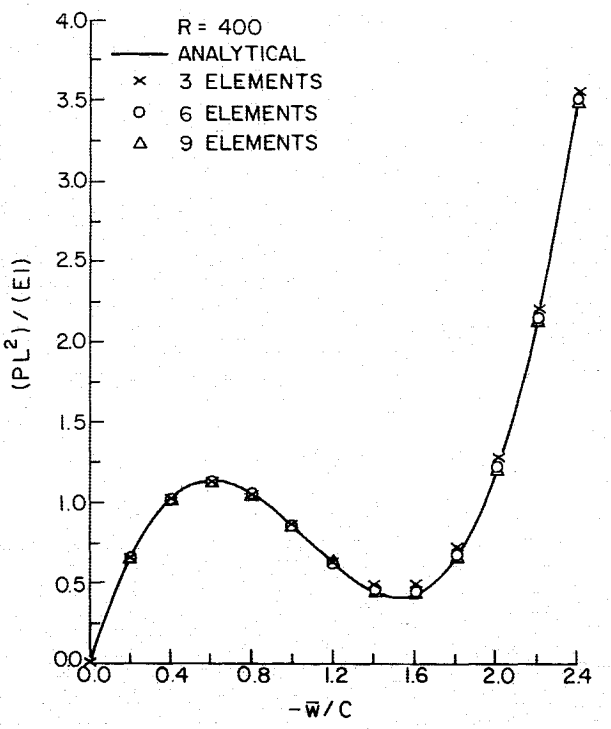

Fig. 17 Nonlinear analysis of a circular arch; linear basis functions, complete under integration; $R = 400$ in.

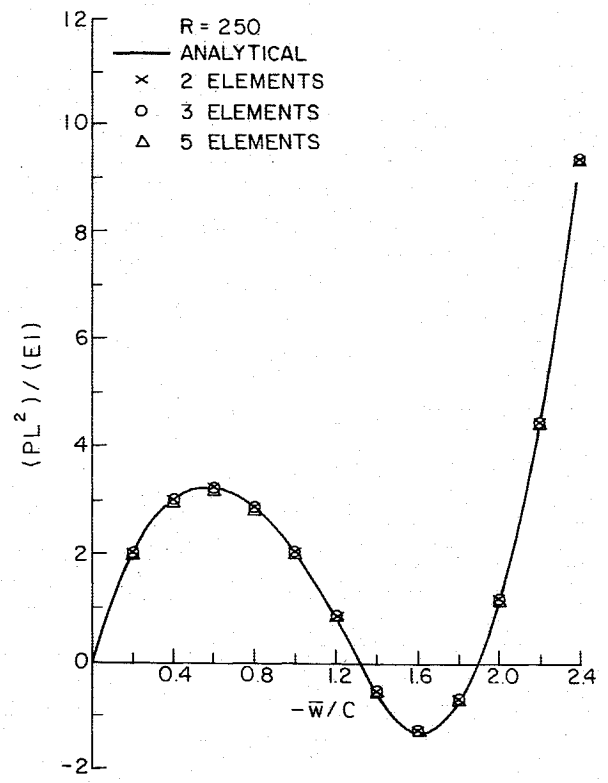

Fig. 16 Nonlinear analysis of a circular arch; quadratic basis functions, complete under integration; $R = 250$ in.

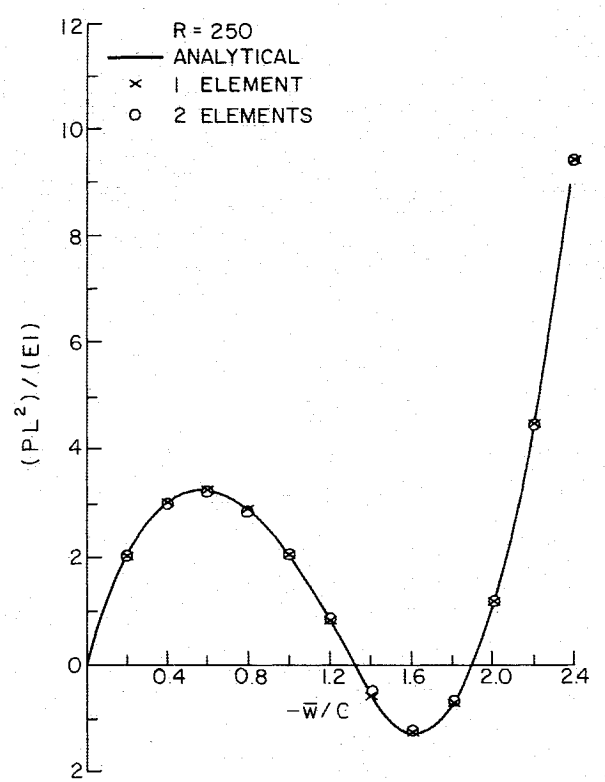

Fig. 18 Nonlinear analysis of a circular arch; cubic basis functions, complete under integration; $R = 250$ in.

rigid-body form of the trigonometric basis functions that was used in the nonlinear problems, and it is apparent from Figs. 12a–12c that these basis functions display excellent accuracy and convergence in these problems. Figures 13–15 show results for the fully integrated quadratic basis function solutions to the arch buckling problem. The fully integrated quadratic elements are included here for comparison because they have the same number of degrees of freedom as the trigonometric elements that are also fully integrated. It may be seen in these figures that the fully integrated quadratic basis functions have comparable accuracy and convergence characteristics as compared to the trigonometric basis functions. The results illustrated in Figs. 16, and similar results for the other geometries that are not presented here, but which may be found in

Heppler and Hansen,[24] indicate that the completely under integrated quadratic basis functions give superior results to the trigonometric basis functions both in terms of accuracy and convergence. It is actually the case, for this set of examples, that the fully reduced integration of the polynomial basis function elements results in superior performance to any of the fully integrated formulations including the trigonometric case. The results presented in Figs. 16–18 illustrate this point very well. Finally, comparable results to those reported in Figs. 13–18 but for different arch geometries may be found in Ref. 24.

Summary and Conclusions

For application to curved and straight Timoshenko beam finite elements, the trigonometric basis functions have been shown to be competitive with polynomial basis functions with regard to accuracy and convergence in both linear and nonlinear problems. At the same time, they are free of shear and membrane locking and have displayed a uniform level of performance in the problems investigated here without recourse to any numerical techniques designed to artificially modify their performance. If the arc-length form of these basis functions is used then there is the added possibility of introducing an additional wave parameter n to enhance the modelling capability of these basis functions. However, it must be noted that, with the exception of straight beams, there is only one value of n that will allow recovery of incremental rigid-body modes in curved beam applications.

References

[1]Hansen, J. S. and Heppler, G. R., "A Mindlin Shell Element Which Satisfies Rigid Body Requirements," *AIAA Journal*, Vol. 23, Feb. 1985, pp. 288–295.

[2]Heppler, G. R., Sharf, I., and Hansen, J. S., "Shell Elements Which Satisfy Rigid Body Requirements," *AIAA/ASME/AHS 26th Structures, Structural Dynamics, and Materials Conference*, Orlando, FL, April 1985, pp. 550–560.

[3]Heppler, G. R., Sharf, I., and Hansen, J. S., "Basis Functions for Axisymmetric Shell Elements Which Satisfy Rigid Body Requirements," *AIAA Journal*, Vol. 24, Dec. 1986, pp. 2014–2021.

[4]Reissner, E., "The Effect of Transverse Shear Deformation on the Bending of Elastic Plates," *Journal of Applied Mechanics*, Vol. 67, No. 2, June 1945, pp. A69–A77.

[5]Goodier, J. N., "Discussion of Reference 4," *Journal of Applied Mechanics*, Vol. 68, No. 3, Sept. 1946, pp. A249–A252.

[6]Reissner, E., "On Bending of Elastic Plates," *Quarterly of Applied Mathematics*, Vol. 5, No. 1, 1947, pp. 55–68.

[7]Mindlin, R. D., "Influence of Rotary Inertia and Shear on Flexural Motions of Elastic Plates," *Journal of Applied Mechanics*, Vol. 18, No. 1, March 1958, pp. 31–38.

[8]Ashwell, D. G. and Sabir, A. B., "Limitations of Certain Curved Finite Elements When Applied to Arches," *International Journal of Mechanical Sciences*, Vol. 13, Feb. 1971, pp. 133–139.

[9]Ashwell, D. G., Sabir, A. B., and Roberts, T. M., "Further Studies in the Application of Curved Finite Elements to Circular Arches," *International Journal of Mechanical Sciences*, Vol. 13, June 1971, pp. 507–517.

[10]Sabir, A. B. and Ashwell, D. G., "A Comparison of Curved Beam Finite Elements When Used in Vibration Problems," *Journal of Sound and Vibration*, Vol. 18, No. 4, 1971, pp. 555–563.

[11]Sabir, A. B. and Lock, A. C., "Large Deflexion, Geometrically Nonlinear Finite-Element Analysis of Circular Arches," *International Journal of Mechanical Sciences*, Vol. 15, Jan. 1973, pp. 37–47.

[12]Dawe, D. J., "Curved Finite Elements for the Analysis of Shallow and Deep Arches," *Computers and Structures*, Vol. 4, No. 3, May 1974, pp. 559–580.

[13]Dawe, D. J., "Numerical Studies Using Circular Arch Finite Elements," *Computers and Structures*, Vol. 4, No. 4, Aug. 1974, pp. 729–740.

[14]Hughes, T. J. R., Taylor, R. L., and Kanoknukulchai, W., "A Simple and Efficient Finite Element for Plate Bending," *International Journal of Numerical Methods in Engineering*, Vol. 11, Oct. 1977, pp. 1529–1543.

[15]Prathap, G. and Bhashyam, G. R., "Reduced Integration and the Shear-Flexible Beam Element," *International Journal of Numerical Methods in Engineering*, Vol. 18, Feb. 1982, pp. 195–210.

[16]Stolarski, H. and Belytschko, T., "Membrane Locking and Reduced Integration in Curved Elements," *Journal of Applied Mechanics*, Vol. 49, No. 1, March 1982, pp. 172–176.

[17]Stolarski, H. and Belytschko, T., "Shear and Membrane Locking in Curved C^0 Elements," *Computer Methods in Applied Mechanics and Engineering*, Vol. 41, No. 3, Dec. 1983, pp. 279–296.

[18]Tabarrok, B., Farshad, M., and Yi, H., "Finite Element Formulation of Spatially Curved and Twisted Rods," *Journal of Computer Methods in Applied Mechanics and Engineering*, (to be published).

[19]Cowper, G. R., "The Shear Coefficient in Timoshenko's Beam Theory," *Journal of Applied Mechanics*, Vol. 33, No. 2, June 1966, pp. 335–340.

[20]Heppler, G. R. and Hansen, J. S., "A Mindlin Element for Thick and Deep Shells," *Computer Methods in Applied Mechanics and Engineering*, Vol. 54, Jan. 1986, pp. 21–47.

[21]Pica, A., Wood, R. D., and Hinton, E., "Finite-Element Analysis of Geometrically Nonlinear Plate Behaviour Using a Mindlin Formulation," *Computers and Structures*, Vol. 11, March 1980, pp. 203–215.

[22]Heppler, G. R., "On the Analysis of Shell Structures Subjected to a Blast Environment: A Finite Element Approach," Univ. of Toronto Institute for Aerospace Studies, Toronto, Ontario, Canada, Rept. 302, Feb. 1986.

[23]Roark, R. J. and Young, W. C., *Formulas for Stress and Strain*, McGraw-Hill, New York, 1975.

[24]Heppler, G. R. and Hansen, J. S., "The Performance of Trigonometric Basis Functions in Timoshenko Beam Finite Elements," *AIAA/ASME/AHS 28th Structures, Structural Dynamics, and Materials Conference, Part I*, AIAA, New York, April 1987, pp. 651–661.

[25]Schreyer, H. L. and Masur, E. F., "Buckling of Shallow Arches," *Journal of Engineering Mechanics Division*, American Society of Civil Engineers, EM4, Vol. 92, Aug. 1966, pp. 1–19.